



Influence of the surface conditions on permeation in the deuterium–MANET system

E. Serra^{*}, A. Perujo

European Commission, Joint Research Centre, Institute for Advanced Materials, Ispra Site, I-21020 Ispra (VA), Italy

Received 6 August 1996; accepted 4 October 1996

Abstract

The condition of the surfaces is of crucial importance for the deuterium permeation through materials. In this work a study of the surface constants for the adsorption (σk_1) and release (σk_2) of deuterium under different surface conditions on the martensitic steel DIN 1.4914 (MANET) has been carried out. The growth of an oxide surface layer (Cr_2O_3) of about 25–30 nm in a MANET sample, heat treated in an oxidizing environment, compared to the bare MANET that have a ‘natural’ oxide of about 5 nm has provoked a reduction of both the permeation rate and the recombination coefficient (about 3 orders of magnitude). In addition, the permeation governing process has changed from diffusion-limited to surface-limited. The measurements of the permeation rate of deuterium were performed by a gas-phase permeation technique over the temperature range 574–746 K and for deuterium driving pressures in the range from 3 to 10^5 Pa.

1. Introduction

The martensitic steel DIN 1.4914 (MArtensitic for NET, MANET) is a Nb bearing steel which has better swelling resistance, lower sensitivity to helium embrittlement and more suitable thermophysical properties than the austenitic stainless steel AISI 316L [1]. MANET is a candidate material for the first wall and structure for the demonstration power reactor DEMO.

The governing deuterium transport and inventory parameters (permeability, diffusivity and solubility) in MANET are well known [2–4] but few data are available for the constants describing surface reactions. In a previous work [5] we obtained the adsorption (σk_1) and recombination (σk_2) constants of deuterium in MANET but unfortunately without being able to control the surfaces of the sample. In the present work the surface conditions of the samples were rigorously controlled. Before and after in-

serting each sample in the permeation apparatus, X-ray photoelectron spectroscopy (XPS) was conducted on both the surfaces of the sample, in order to evaluate the composition and to determine the thickness of the oxide layer on the surfaces.

In fusion reactor technology, great emphasis is made on tritium behaviour because of the implications for the efficiency of the reactor fuel cycle and because of the possible radiological hazards associated with tritium. The knowledge of the release rate of hydrogen and/or its isotopes from the surface and the rate at which atoms move into the subsurface layer is required in order to evaluate the recycling of hydrogen; to evaluate and control tritium retention in walls when operated with deuterium/tritium plasmas; and to quantify the hazard problems of tritium permeation [6]. Numerical codes have been developed for the calculation of inventory, permeation and recycling of deuterium and tritium in fusion reactor design concepts in non-steady state conditions [7–11]. This permits evaluation and control of tritium retention in walls and structures when operated with deuterium/tritium plasmas. The codes utilize, as essential input data, either the hydrogen trans-

^{*} Corresponding author. Fax: +39-332 785 835.

port and inventory parameters or/and the surface constants of the fusion reactor candidate materials.

2. Experimental

The material studied was MANET II, a development of MANET [12]. The MANET II samples consisted of discs 48 mm in diameter and 0.5 mm in thickness. They were machined from a slab of material supplied by Kernforschungszenrum Karlsruhe from the Net-heat (No. 50803) with the following composition (wt%): C, 0.11; Cr, 10.3; Ni, 0.65; Mo, 0.58; V, 0.19; Nb, 0.14; Si, 0.18; Mn, 0.85; S, 0.004; P, 0.005; B, 0.0072; N, 0.030; Al, 0.012; Co, 0.006; Cu, 0.010; Zr, 0.014; Zn, 0.001; Sb, 0.0004; As, 0.010 and Fe, balance. The membranes underwent the following heat treatment in order to produce a fully 6-ferri-rite free martensitic phase: heating at 1243 K for 2 h, austenizing at 1348 K for 0.5 h, quenching to room temperature, tempering at 1023 K for 2 h and slow cooling to room temperature.

The method chosen for the high pressure (0.1 to 100 kPa) measurements during the current investigation is a gas-phase technique where, after evacuating the apparatus to an ultra high vacuum so that both sides of a sample are initially in contact with vacuum, one side of the sample (the 'high pressure side') is instantaneously exposed to deuterium gas at a known, fixed pressure. Gas permeates through the sample and is released at the other side (the 'low pressure side'), where it causes a pressure rise in an initially evacuated, calibrated volume. The pressure rise is measured using a Baratron capacitance manometer with a full scale reading of 100 Pa (1 mbar). Since the volume is calibrated, either the pressure rise could be converted into an amount of gas in moles permeating through unit area of the sample ($Q(t)$) or the rate of pressure rise could be converted into an amount of gas in moles permeating through unit area of the sample per second ($J(t)$).

The apparatus is constructed from standard stainless steel UHV components [5]. Bakeout of the entire system is possible using heating tapes. Residual pressures lower than 10^{-6} Pa (10^{-8} mbar) prior to system bakeout at 573 K and less than 10^{-7} Pa afterwards are obtained before any experiment. High pressure deuterium gas, with a nominal purity of 99.7%, is taken from a cylinder and admitted to the sample via two pressure controllers which enable the pressure to be set at any value between 0.1–150 kPa (1.0 to 1500 mbar). The sample is heated by a resistance furnace and the temperature may be set at values up to 773 K by a temperature controller with a thermocouple held in a well, drilled into one of the flanges holding the sample, allowing a temperature stability of ± 1 K. An analysis of the high pressure gas and the permeated gas is made with a quadrupole mass spectrometer. Thus it is possible to check for possible contaminants and to distinguish permeation from outgassing. The volume of the low pressure side of

the sample is measured by a gas expansion method (Sieverts' method) using a calibrated volume (9.13×10^{-5} m³) which is permanently attached to the apparatus.

The measurements in the range of deuterium pressure of 3–100 Pa were performed by a 'reverse permeation technique'. For this, gas is allowed to permeate through the sample into the 'low pressure side' in the usual way. When the pressure in the 'low pressure side' reaches the required pressure for the measurement, the 'high pressure side' is evacuated and kept under vacuum. Permeation occurs in the reverse direction to the measurements described above, resulting in a pressure decrease in the 'low pressure side'. As before, the rate of pressure change which in this case is a decrease (measured using the Baratron) can be converted into an amount of gas permeating through unit area of the sample per second. Thus permeation measurements can be made over a wide range (nearly 5 decades) of pressure, making efficient use of equipment and experimental time. The reliability of the low pressure measurements depends on the assumption that the pressure decrease is predominantly due to the permeation through the MANET disc and not through any other part of the apparatus. When investigating a thin sample of MANET, which has a relatively high permeability this assumption is reasonable. In addition, a check on the consistency of the low pressure data with the high pressure measurements is made in order to show that there is no discontinuity in the data across the whole pressure range investigated.

A microcomputer interfaced to the equipment via a digital voltmeter is used for data storage and later processing.

3. Theory

It is well known that the hydrogen isotopes permeation rate through a membrane in the stationary condition, can be described by simple analytical equations for the two extreme cases, i.e., the diffusion limited and the surface limited regimes. In the more general case, a general equation describing the permeating flux, J , as a function of the driving pressure, p , in both regimes and also in the intermediate domain is needed. In this work we follow the approach of Ref. [13] and that has been explicitly described in a previous paper [5]. The only difference in the experimental data treatment in this work as compared with that of Ref. [5] is the expression used to fit the variation of the ratio J/J_i with W^2 to obtain the adsorption constant. The expression used in this work is given by

$$\log\left(\frac{J}{J_i}\right) = \left[\frac{\sum_{n=0}^5 a_n (\ln W^2)^n}{\sum_{n=0}^5 b_n (\ln W^2)^n} \right], \quad (1)$$

with $a_0 = -0.5314$, $a_1 = -0.0927$, $a_2 = -0.01828$, $a_3 = -0.00126$, $a_4 = -5.4621 \times 10^{-5}$, $a_5 = -8.201 \times 10^{-7}$, $b_0 = 1$, $b_1 = 0.011$, $b_2 = 0.011295$, $b_3 = 1.7448 \times 10^{-5}$, $b_4 = 8.9754 \times 10^{-6}$ and $b_5 = -4.666 \times 10^{-8}$, fits the theoretical curve with $\%ERR (W^2) = 100 \text{ abs}[(J/J_{\text{th}}) - (J/J_{\text{fit}})/(J/J_{\text{th}})] (10^{-9} \ll W^2 \ll 10^{14})$ less than 0.5%.

4. Results and discussion

In alloys like stainless steel or MANET, active elements such as chromium or aluminium are added, which, since they have a more negative free energy for oxidation than the other main constituents of the alloy, form a continuous surface layer ('natural' oxide) which protects the alloy from further oxidation. It is possible to grow oxide layers on these steels under a variety of conditions. The rate at which each stage of the oxidation process is reached and proceeds is governed by many factors such as the alloy composition, the oxidation temperature and the partial pressure of oxygen in contact with the metal surface. For instance it is known that if oxidation continues for long enough time, spalling or cracking of the scale may occur because of stresses set up at the scale/metal interface from the changes in crystal dimensions on oxidation.

In this work the best result, in terms of production of a permeation barrier by the growth of oxide layers on MANET II has been reached oxidizing in an environment of 'wet hydrogen'. It was obtained with a MANET II disc heated for 72 h in an environment consisting of 10^5 Pa of H_2 with about 1000 vppm of H_2O to get the oxide layer. It is worth noticing that controlled oxidation could represent a convenient way to produce permeation barriers because of good thermo-mechanical stability of the oxide layer compared to those obtained by other techniques like chemical vapour deposition (CVD) or vacuum plasma spray (VPS), which could lead to problems related to the stability of the bond between the substrate and the coating, especially at high temperatures.

The variation with pressure of the steady state flux J and of the flux/pressure ratio J/p , over the membranes temperature range 746–574 K, for deuterium, is shown in Figs. 1 and 2. In these figures, a comparison is shown between the bare and the oxidized MANET II samples.

Both sides of the bare disc of MANET II were mechanically polished before its insertion into the permeation measuring equipment; thus only 'natural oxide' layers resulting from exposure to air should be present on the surfaces. Occasionally during the permeation measurements, a small decrease of permeability and diffusivity values was noted, especially at the highest temperature studied (743 K). Every time this phenomenon (probably due to a build-up of an oxide on the surface during the permeation measurements) has been observed, the sample

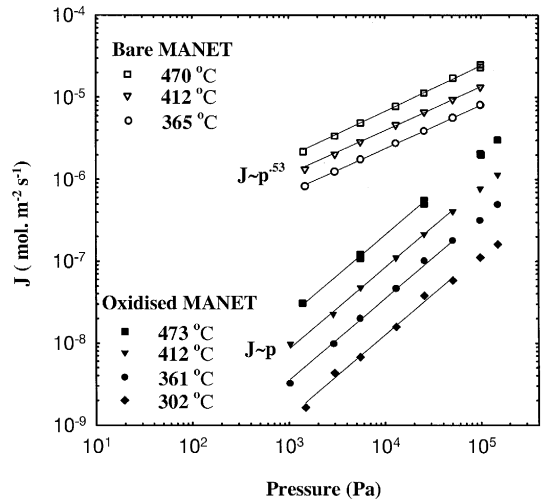


Fig. 1. The permeation rate through oxidised MANET II and bare MANET II versus pressure.

has been taken out of the rig and both its sides have been mechanically polished.

In the pressure range 1500– 10^5 Pa (Fig. 1), a half-power pressure dependence (diffusion-limited permeation) of the permeation flux for the bare MANET II was observed, whereas it is obvious that permeation is surface limited at pressures less than 5×10^4 Pa for the oxidized MANET II. From these data, values of the adsorption constant σk_1 were obtained using Eq. (1). The Arrhenius plot of σk_1 for deuterium for the bare and oxidized MANET II is compared with other work in Fig. 3. The constant of

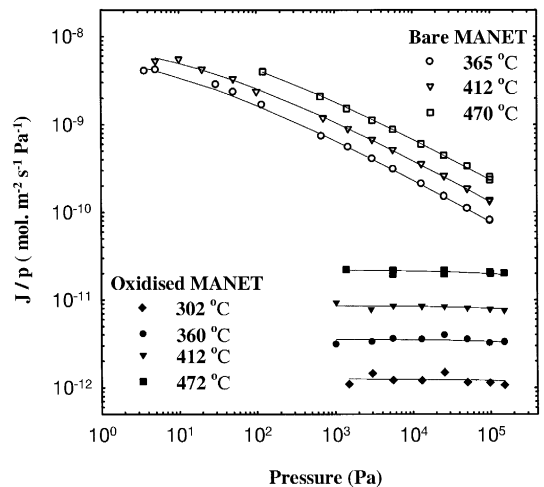


Fig. 2. The permeation rate divided by the pressure (J/p) versus pressure for oxidized MANET II and bare MANET II. The fitted lines are calculated using Eq. (1).

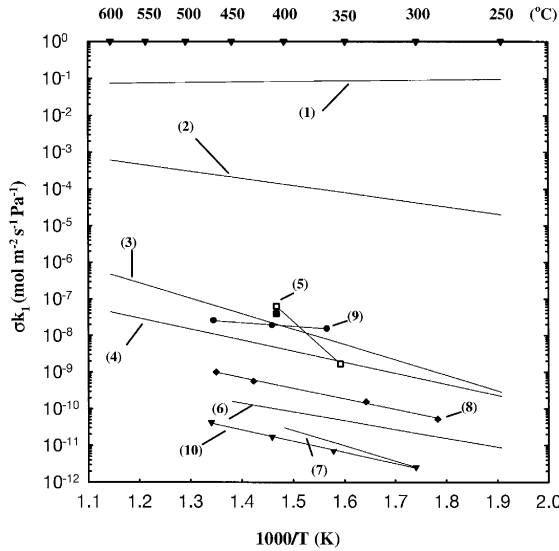


Fig. 3. Variation of measured surface rate constant σk_1 , with reciprocal temperatures, compared to published data. (1) and (2) Pick and Sonnenberg [18] model and Baskes [14] model respectively for MANET II (with sticking factor $s = 1$, and $\sigma = 1$); (3) H_2 , 316 SS ion beam cleaned (Grant et al. [15]); (4) H_2 , 316 SS oxidized both surfaces (Grant et al. [15]); (5) H_2 , St 60 (Ali-Khan et al. [13]) (the filled symbol is for D_2); (6) D_2 , Inconel 600 (Rota et al. [16]); (7) D_2 , 304 SS (Braun et al. [17]); (8) D_2 MANET II (Serra and Perujo [5]); (9) and (10) bare and oxidized MANET II respectively (this work).

recombination for oxidized MANET II, σk_2 , was determined using: $k_2 = k_1/K_S^2$ (eq. (8) in Ref. [5]). The Arrhenius expressions for bare MANET II for the deuterium permeability (373–743 K), diffusivity D and Sieverts' constant values K_S (633–743 K) are taken from Refs. [4,23]:

$$\Phi = 4.2 \times 10^{-8} \exp\left(-\frac{42380}{RT}\right) \quad (\text{mol m}^{-1} \text{s}^{-1} \text{Pa}^{-1/2})$$

$$D = 1.01 \times 10^{-7} \exp\left(-\frac{13210}{RT}\right) \quad (\text{m}^2 \text{s}^{-1})$$

$$K_S = 0.27 \exp\left(-\frac{26670}{RT}\right) \quad (\text{mol m}^{-3} \text{Pa}^{-1/2}). \quad (2)$$

The Arrheniusplot of σk_2 of deuterium for bare and oxidized MANET II is compared with other works in Fig. 4. The Arrhenius expression surface constants of MANET II for deuterium, σk_1 and σk_2 , are as follows:

Bare MANET II

$$\sigma k_1 = 5.56 \times 10^{-7} \exp\left(-\frac{19093}{RT}\right) \quad (\text{mol m}^{-2} \text{s}^{-1} \text{Pa}^{-1})$$

$$\sigma k_2 = 7.63 \times 10^{-6} \exp\left(+\frac{34247}{RT}\right) \quad (\text{mol}^{-1} \text{m}^4 \text{s}^{-1}). \quad (3)$$

Oxidized MANET II

$$\sigma k_{1(\text{ox})} = 4.9 \times 10^{-7} \exp\left(-\frac{58383}{RT}\right) \quad (\text{mol m}^{-2} \text{s}^{-1} \text{Pa}^{-1})$$

$$\sigma k_{2(\text{ox})} = 6.7 \times 10^{-6} \exp\left(-\frac{5044}{RT}\right) \quad (\text{mol}^{-1} \text{m}^4 \text{s}^{-1}), \quad (4)$$

where $R = 8.314 \text{ J K}^{-1} \text{ mol}^{-1}$ and T is the temperature in Kelvin.

Baskes [14] and Pick and Sonnenberg [18] have estimated the constant of recombination, k_2 , theoretically:

$$k_2 = \frac{2Cs}{(2mT)^{1/2}} \frac{1}{K_{SO}^2} \exp\left(\frac{2E_S - E_x}{RT}\right) \quad [14],$$

$$k_2 = \frac{Cs}{(2mT)^{1/2}} \frac{1}{K_{SO}^2} \exp\left(\frac{2E_S}{RT}\right) \quad [18], \quad (5)$$

with $C = 4.376 \text{ mol K}^{1/2} \text{ u}^{1/2} \text{ Pa}^{-1} \text{ m}^{-2} \text{ s}^{-1}$; s = sticking coefficient; m = mass of the diffusing atom (u); $E_x = \max(0, E_s + E_d)$; E_d and E_s are the activation energies for the diffusivity and solubility, respectively, and K_{SO} is the pre-exponential factor in the Arrhenius equation for the deuterium Sieverts' constant.

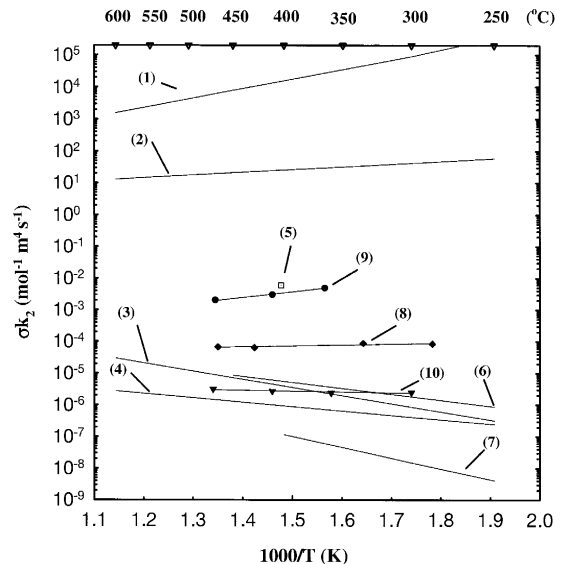


Fig. 4. Variation of measured surface rate constant σk_2 , with reciprocal temperatures, compared to published data. (1) and (2) Pick and Sonnenberg [18] model and Baskes [14] model respectively for MANET II (with sticking factor $s = 1$, and $\sigma = 1$); (3) H_2 , 316 SS ion beam cleaned (Grant et al. [15]); (4) H_2 , 316 SS oxidized both surfaces (Grant et al. [15]); (5) H_2 , St 60 (Ali-Khan et al. [13]); (6) D_2 , Inconel 600 (E. Rota et al. [16]); (7) D_2 , 304 SS (Braun et al. [17]); (8) D_2 MANET II (Serra and Perujo [5]); (9) and (10) bare and oxidized MANET II respectively (this work).

The difference between the Pick and Sonnenberg [18] and Baskes [14] models is discussed by Causey and Baskes [19] and Richards [20]. Using the values of E_d , E_s and K_{s0} from Eq. (2), the k_2 and k_1 ($k_1 = k_2 K_S^2$) constants for the two models were obtained and are shown in Figs. 3 and 4, respectively. The values of the activation energy of the recombination constant k_2 are $-53\,300$ and $-13\,500$ J mol $^{-1}$ ($k_i = k_{oi} \exp(-Q_i/RT)$) for the Pick and Sonnenberg model and the Baskes model, respectively. The difference between the k_2 values from the two models and the recombination constant measured in this work for bare MANET II can be explained by assuming two sticking coefficients: $s_{PS} = 7 \times 10^{-6} \exp(-19\,100/RT)$ and $s_B = 3 \times 10^{-6} \exp(+20\,800/RT)$ for the Pick and Sonnenberg model and Baskes model, respectively. The sticking probability s is the probability that a hydrogen molecule impinging on the surface will dissociate and that the resulting hydrogen atoms will stick to the surface in chemisorption sites. The difference between the experimental values for bare MANET II and the theoretical values is due to the presence of the 'natural' oxide layer of the steel. This layer yields a non-zero activation barrier for dissociation $2E_c$.

As mentioned above, for oxidized MANET II, the governing process is the recombination at the surface (see Fig. 1), and the permeation rate is independent of the thickness of the membrane. The diffusion in the oxide cannot be considered rate limiting because the oxide thickness is only 0.006% of the bulk (30 nm compared with 0.5 mm). It is worth noticing that in the blanket concept of DEMO the calculated tritium partial pressure in the blanket is less than 10^4 Pa [21]. The presence of the oxide layer on the surface of MANET II produces a reduction of the recombination coefficient of about three orders of magnitude and an increase of the energy of activation for recombination from $-34\,247$ (for the bare MANET II) to 5044 J mol $^{-1}$ (for the oxidized MANET II). This means that, in terms of the Pick and Sonnenberg model, there is an increase of the activation barrier for dissociation ($2E_c$) from $19\,100$ (for the bare MANET II) to $58\,383$ J mol $^{-1}$ (for the oxidized MANET II). Our measurements seem to indicate that the Pick and Sonnenberg model might describe better the surface recombination constant because it involves an activated process for dissociation ($2E_c > 0$).

To confirm and characterize the growth of the oxide layer on the MANET II specimen heated for 72 h in an environment consisting of 10^5 Pa of H_2 with about 1000 vppm of H_2O , X-ray photoelectron spectroscopy (XPS) measurements were conducted on both the untreated (bare MANET II) and heat treated (oxidized MANET II) specimen. The XPS analysis was carried out from 0 to 45 nm at 5 nm intervals of the surfaces of both the samples, in order to reveal the composition at different depths of the surfaces. At the top of both surfaces Cr was in the form of Cr_2O_3 and also Fe was in the form of Fe_2O_3 . At 5 nm, in the bare MANET II, Cr was both Cr_2O_3 and Cr (metallic) and Fe was only metallic. In Fig. 5(a), (b) are depicted the

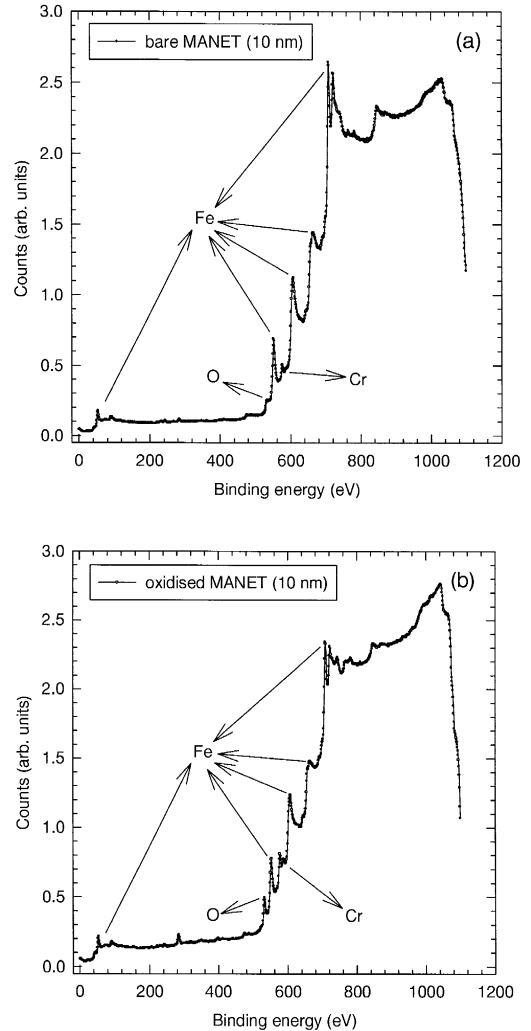


Fig. 5. XPS spectrum at 10 nm, (a) for the bare MANET II and (b) for the oxidized MANET II, respectively.

XPS spectrum, at 10 nm, for the bare MANET II and oxidized MANET II, respectively. The Fe, Cr and O photopeaks were detected in the spectra. The composition, at 10 nm, were O = 10.8 at.%, C = 10.2 at.%, Cr = 4.3 at.% and Fe = 74 at.% for the bare MANET II and O = 17.3 at.%, C = 20.1 at.%, Cr = 12.3 at.% and Fe = 50.3 at.% for the oxidized MANET II. The region with the binding energy 565 to 595 eV, corresponding to the Cr doublet, has been enlarged and is shown in Fig. 6(a) (bare MANET II) and Fig. 6(b) (oxidized MANET II). From the shape and the splitting in energy of the Cr doublet, it is possible to state that, in the bare MANET II, Cr is metallic whereas, in the oxidized MANET II, it is in the form of Cr_2O_3 . In the oxidized MANET II Cr is in the form of Cr_2O_3 down to 25–30 nm. Below 30 nm, the photopeaks of both samples were the same and Fe and Cr were

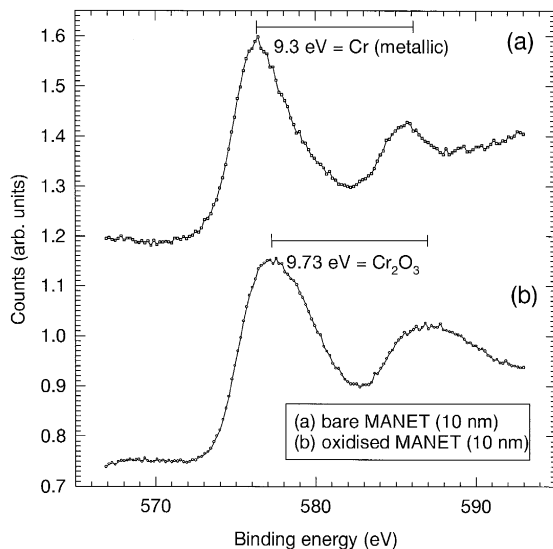


Fig. 6. Enlarged region with binding energy from 565 to 595 eV (Cr doublet) for (a) bare MANET II and (b) oxidized MANET II.

metallic. This result strongly confirms the build up of an superimposed oxide surface layer of Cr_2O_3 of about 25–30 nm in the MANET II sample heat treated in an oxidizing environment, compared to the bare MANET II that has a ‘natural’ oxide of about 5 nm.

Other authors [22] have found that after a heat treatment of 10 h, at 900 K, in presence of 10^5 Pa of hydrogen with 0.8 vppm of H_2O , 0.1 vppm of O_2 , 0.01 vppm of CO_2 and 0.1 vppm of CH_4 , the diffusivity of MANET II was greatly reduced (about 2–3 orders of magnitude) and that Cr_2O_3 and MnO_x oxides or spinel ($\text{Cr}_x\text{Mn}_y\text{O}_4$) were found in the surface. This confirms that the oxide formation strongly depends on the treatment conditions. The composition of the oxide layer is drastically affected by the oxygen partial pressure during the heat treatment. In general, it was found that, the lower the oxygen potential, the less Fe is included in the oxide layer. This is a possible explanation because, in the present work, the best result was reached in an environment of ‘wet hydrogen’.

5. Conclusion

Constants of adsorption and recombination σk_1 and σk_2 of deuterium on martensitic steel DIN 1.4914 have been determined under different, well characterized, surface conditions. It was found that the condition of the surfaces is of crucial importance for the hydrogen permeation through this steel. The growth of an oxide surface layer (Cr_2O_3) of about 25–30 nm in a MANET II sample heat treated in an oxidizing environment, compared to the bare MANET II that have a ‘natural’ oxide of about 5 nm has provoked a reduction of both the permeation rate and the recombination coefficient (about three orders of magnitude). In addition, the permeation governing process has

changed from diffusion-limited to surface-limited. In the previous work [5], the values of adsorption and recombination σk_1 and σk_2 of deuterium on MANET II were between the values of the bare and oxidized MANET II presented here (Figs. 3 and 4), indicating that the thickness of the oxide surface layers in those samples were between 5 and 25 nm.

Acknowledgements

The authors would like to thank Mr L.G. Mammarella for XPS analysis.

References

- [1] R.L. Klueh, K. Ehrlich and F. Abe, *J. Nucl. Mater.* 191–194 (1992) 116.
- [2] K.S. Forcey, D.K. Ross, J.C.B. Simpson and D.S. Evans, *J. Nucl. Mater.* 160 (1988) 117.
- [3] F. Reiter, S. Alberici, J. Camposilvan, E. Serra, K.S. Forcey and A. Perujo, *Z. Phys. Chem.* 181 (1993) 151.
- [4] E. Serra, A. Perujo and K.S. Forcey, Influence of Traps on Deuterium Diffusion in the Martensitic Steel DIN 1.4914 MANET, to be published.
- [5] E. Serra and A. Perujo, *J. Nucl. Mater.* 223 (1995) 157.
- [6] K.J. Dietz, F. Waelbroeck and P. Wienhold, *Jül-1448* (1977).
- [7] M.I. Baskes, *SAND 83-8231* (1983).
- [8] P. Wienhold, M. Profant, F. Waelbroeck and J. Winter, *Jül-1825* (1983).
- [9] W. Mdller, *IPP 9/44* (1983).
- [10] G. Gervasini and F. Reiter, *J. Nucl. Mater.* 155–157 (1988) 754.
- [11] G.R. Longhurst, D.F. Holland, J.L. Jones and B.J. Merrill, *TMAP4 User's Manual*, EGG-FSP-10315 (1992).
- [12] K. Anderko, K. Ehrlich, L. Schaefer and M. Schirra, *KfK-5060* (1993).
- [13] I. Ali-Khan, K.J. Dietz, F. Waelbroeck and P. Wienhold, *J. Nucl. Mater.* 76&77 (1978) 337.
- [14] M.I. Baskes, *J. Nucl. Mater.* 92 (1980) 318.
- [15] D.M. Grant, D.L. Cummings and D.A. Blackburn, *J. Nucl. Mater.* 152 (1988) 139.
- [16] E. Rota, F. Waelbroeck, P. Wienhold and J. Winter, *J. Nucl. Mater.* 111&112 (1982) 233.
- [17] M. Braun, B. Emmoth, F. Waelbroeck and P. Wienhold, *J. Nucl. Mater.* 93&94 (1980) 861.
- [18] M.A. Pick and K. Sonnenberg, *J. Nucl. Mater.* 131 (1985) 208.
- [19] R.A. Causey and M.I. Baskes, *J. Nucl. Mater.* 145–147 (1987) 284.
- [20] P.M. Richards, *J. Nucl. Mater.* 152 (1988) 246.
- [21] F. Reiter, S. Tominetti and Perujo, *Fusion Eng. Des.* 15 (1992) 223.
- [22] S. Alberici, PhD thesis, Politecnico di Torino (1995).
- [23] A. Perujo, E. Serra, S. Alberici, S. Tominetti and J. Camposilvan, Hydrogen in the martensitic DIN 1.4914: A review, Proc. Int. Symp. on Metal Hydrogen Systems: Fundamentals and Applications, Les Diablerets, Switzerland, Aug. 25–30 (1996), *J. Alloy Compounds*, to be published.